Exploring impact of supersaturated lipid-based drug delivery systems of celecoxib on in vitro permeation across Permeapad membrane and in vivo absorption

Ilie, Alexandra Roxana; Griffin, Brendan T.; Brandl, Martin; Bauer-Brandl, Annette; Jacobsen, Ann Christin; Vertzoni, Maria; Kuentz, Martin; Kolakovic, Ruzica; Holm, René

Published in:
European Journal of Pharmaceutical Sciences

DOI:
10.1016/j.ejps.2020.105452

Publication date:
2020

Document Version
Publisher's PDF, also known as Version of record

Citation for published version (APA):
Ilie, A. R., Griffin, B. T., Brandl, M., Bauer-Brandl, A., Jacobsen, A. C., Vertzoni, M., Kuentz, M., Kolakovic, R., & Holm, R. (2020). Exploring impact of supersaturated lipid-based drug delivery systems of celecoxib on in vitro permeation across Permeapad membrane and in vivo absorption. *European Journal of Pharmaceutical Sciences*, *152*, Article 105452. https://doi.org/10.1016/j.ejps.2020.105452

European Journal of Pharmaceutical Sciences 152 (2020) 105452

Contents lists available at ScienceDirect

European Journal of Pharmaceutical Sciences

journal homepage: www.elsevier.com/locate/ejps

Exploring impact of supersaturated lipid-based drug delivery systems of celecoxib on *in vitro* permeation across Permeapad® membrane and *in vivo* absorption

Alexandra-Roxana Ilie[a,b], Brendan T. Griffin[b,*], Martin Brandl[c], Annette Bauer-Brandl[c], Ann-Christin Jacobsen[c], Maria Vertzoni[d], Martin Kuentz[e], Ruzica Kolakovic[a], René Holm[a,f]

[a] Drug Product Development, Janssen Research and Development, Johnson & Johnson, Beerse, Belgium
[b] School of Pharmacy, University College Cork, Cork, Ireland
[c] Department of Physics, Chemistry and Pharmacy, University of Southern Denmark, Odense, Denmark
[d] Department of Pharmacy, National and Kapodistrian University of Athens, Zografou, Greece
[e] University of Applied Sciences and Arts Northwestern Switzerland, Institute of Pharma Technology, Muttenz, Switzerland
[f] Department of Science and Environment, Roskilde University, 4000 Roskilde, Denmark

ARTICLE INFO

Keywords:
Supersaturated lipid-based drug delivery systems
Drug permeability
Steady-state flux
Dynamic permeation model
In vivo pharmacokinetics

ABSTRACT

Supersaturated lipid-based drug delivery systems have recently been investigated for oral administration for a variety of lipophilic drugs and have shown either equivalent or superior oral bioavailability compared to conventional non-supersaturated lipid-based drug delivery systems. The aim of the present work was to explore supersaturated versus non-supersaturated lipid-based systems at equivalent lipid doses, on *in vivo* bioavailability in rats and on *in vitro* permeation across a biomimetic Permeapad® membrane to establish a potential *in vivo - in vitro* correlation. A secondary objective was to investigate the influence of lipid composition on *in vitro* and *in vivo* performance of lipid systems. Results obtained indicated that increasing the celecoxib load in the lipid-based formulations by thermally-induced supersaturation resulted in increased bioavailability for medium and long chain mono-/di-glycerides systems relative to their non-supersaturated (i.e. 85%) reference formulations, albeit only significant for the medium chain systems. Long chain systems displayed higher celecoxib bioavailability than equivalent medium chain systems, both at supersaturated and non-supersaturated drug loads. *In vitro* passive permeation of celecoxib was studied using both steady-state and dynamic conditions and correlated well with *in vivo* pharmacokinetic results with respect to compositional effects. In contrast, permeation studies indicated that flux and percentage permeated of supersaturated systems, either at steady-state or under dynamic conditions, decreased or were unchanged relative to non-supersaturated systems. This study has shown that by using two cell-free Permeapad® permeation models coupled with rat-adapted gastro-intestinal conditions, biopredictive *in vitro* tools can be developed to be reflective of *in vivo* scenarios. With further optimization, such models could be successfully used in pharmaceutical industry settings to rapidly screen various prototype formulations prior to animal studies.

Abbreviation list

4-BBBA	4-bromophenyl-boronic acid
A/V	Area-to-volume ratio
ACN	Acetonitrile
aDS	Apparent degree of saturation
ANOVA	Analysis of variance
AUC	Area under the plasma concentration-time curve
CCX	Celecoxib
C_{max}	Maximum plasma concentration
GI	Gastro-intestinal
IBU	Ibuprofen
IVIVC	*In vitro-in vivo* correlations
LBDDS	Lipid-based drug delivery systems
LC	Long chain
LCM	Long chain mono-/di-glycerides
MC	Medium chain
MCM	Medium chain mixed glycerides

* Corresponding author.
E-mail address: Brendan.griffin@ucc.ie (B.T. Griffin).

https://doi.org/10.1016/j.ejps.2020.105452
Received 3 June 2020; Received in revised form 1 July 2020; Accepted 1 July 2020
Available online 03 July 2020

PS80	Polysorbate 80
PWSDs	Poorly water-soluble drugs
RP-UPLC	Reversed-phase Ultra Performance Liquid Chromatography (UPLC™)
rSIF	Rat simulated intestinal fluid
S	Surfactant
S_{eq}	Equilibrium solubility
sLBDDS	Supersaturated lipid-based drug delivery systems
t_{max}	Time to reach maximum plasma concentration

1. Introduction

With numerous commercial successes, lipid-based drug delivery systems (LBDDS) have a proven track record to improve oral absorption of poorly water-soluble drugs (PWSDs) through a variety of mechanisms including increasing solubility, reducing food-induced exposure variability and improving overall intestinal uptake (Savla et al., 2017). To-date the merits of LBDDS have been limited to a relatively small number of highly lipophilic drugs, and a key drawback is that the dose of drug that can be loaded in LBDDS is hindered by the drug solubility in lipids (Thomas et al., 2012; Michaelsen et al., 2016). The need to administer high doses of PWSDs by the oral route, such as in pre-clinical safety and toxicological evaluation, has expanded the potential for use of supersaturated lipid-based drug delivery systems (sLBDDS) (Siqueira Jørgensen et al., 2018). While risks of insufficient stability on long term storage remain a challenge to successful exploitation of sLBBDS as clinical formulations, a recent study has demonstrated that stability of selected sLBDDS is suitable for a preclinical setting to maximise drug exposure (Ilie et al., 2020a). Pharmacokinetic studies involving sLBDDS have indicated an improved *in vivo* performance relative to conventional non-supersaturated LBDDS or aqueous suspension for a range of either weakly basic or neutral drugs including halofantrine (Thomas et al., 2012; Michaelsen et al., 2016), simvastatin (Thomas et al., 2013), fenofibrate (Thomas et al., 2014) and R3040 (Siqueira Jørgensen et al., 2018) in different preclinical species (i.e. rat, dog and mini-pig). The most commonly described preparation method for sLBDDS is heating the drug together with the lipid excipients to 50–60°C, followed by cooling to ambient temperature. To-date the vast majority of these studies have used a well characterized lipid-surfactant-co-solvent mixture (i.e. Soybean oil + Maisine CC or Captex 300 + Capmul MCM (55%) as lipid components, Kolliphor RH40 (35%) and ethanol (10%), w/w%) as the delivery vehicle. However, given the compositional complexity of this specific LBDDS, involving three lipidic excipients plus a co-solvent, it would be preferable to consider less complex LBDDS that can be rapidly screened in an industrial drug development setting (Holm, 2019; Savla et al., 2017; Müllertz et al., 2010).

Various *in vitro* tools are commonly used for biopharmaceutical characterisation of prototype formulations, with an increasing focus on developing *in vitro* tests that are predictive of or at least provide mechanistic insights into the critical steps involved in oral absorption *in vivo*. For LBDDS, a range of *in vitro* dilution, dispersion and dynamic (gastro-)intestinal (GI) lipolysis tests with pH-titration have been employed (Griffin et al., 2014; Kleberg et al., 2014; Berthelsen et al., 2019). Optimization of biorelevant media to match the rats GI conditions (i.e. lower enzymatic activity and dilution volumes, higher bile salt and lipid concentrations) have proven useful to predict the *in vivo* performance in a two-stage GI *in vitro* model of furosemide (Christfort et al., 2019), in *silico* models (Berghausen et al., 2016), and in two digestion models using danazol or R3040 LBDDS (Anby et al., 2014; Siqueira Jørgensen et al., 2018).

Despite the advances in optimising digestion conditions to more closely match the *in vivo* scenario, overall a limited number (50%) of *in vitro-in vivo* correlations (IVIVC) have been observed for LBDDS based on comparing drug solubilisation in the aqueous phase of the digestion medium from the standard *in vitro* lipolysis model and the *in vivo* drug absorption (Feeney et al., 2016). As a result, the focus has shifted toward exploration of models that simultaneously assess the interplay between digestion and drug permeation by incorporating a permeation compartment in the classical digestion models (Buckley et al., 2013). In addition, there is a need to advance models that mechanistically can explore the interplay between free drug (i.e. molecularly dissolved) and drug bound as its colloidal associates, given it has been suggested that free drug can permeate across biological or artificial membranes, whereas drug solubilised within colloidal species may not (Williams et al., 2013b; Berben et al., 2018). Several studies have shown that the concentration of molecularly dissolved drug provides the driving force for absorption while using different solubilising agents: non-ionic surfactants (Fischer et al., 2011a; Fischer et al., 2011b), cyclodextrins (Dahan et al., 2010) or bile-salt micelles in simulated intestinal fluid (Frank et al., 2012). Berthelsen *et al.* have recently compared six combined digestion-permeation models, underlining the potential for an improved IVIVC using either the cell-free biomimetic membrane Permeapad® or the Caco-2 cell monolayers as permeation barriers (Berthelsen et al., 2019). Specifically, Keemink and co-workers developed a two-compartment model to simultaneously study the digestion-permeation interplay using Caco-2 cell monolayers in a cone-shaped digestion vessel (Keemink et al., 2019). Thus, the two-stage model correctly predicted the rank order of the *in vivo* performance in pigs of three fenofibrate LBDDS and the carvedilol absorption in dogs after administration as dissolved in LBDDS or co-administered with LBDDS (Keemink et al., 2019; Griffin et al., 2014; Alskär et al., 2019). While the use of the integrated Caco-2 based model has demonstrated impressive results, it should also be acknowledged that the complexity of this experimental setup limits its more widespread application as a screening tool in the pharmaceutical industry. Another mechanism to mimic absorption of drug in the intestine is via the use of an organic layer, such as octanol or decanol, as part of the *in vitro* setup. Recently, O'Dwyer and co-workers proposed a two-stage biphasic lipolysis setup, incorporating a gastric-to-intestinal transition with a layer of decanol acting as an absorptive compartment. This setup was tested using LBDDS containing three model drugs (nilotinib, fenofibrate and danazol) and was found to more reliably predict *in vivo* bioavailability compared to the standard pH-stat method (O'Dwyer et al., 2020).

Alternatively, the biomimetic artificial barrier, Permeapad®, offers a cell-free approach to screen formulations in a simultaneous digestion-permeation model (Bibi et al., 2017). Permeapad® consists of a phosphatidylcholine layer immobilized between two cellulose-based support sheets, which has been used to evaluate drug (passive) permeability and to screen drug formulations (Di Cagno et al., 2015; Bibi et al., 2017; Jacobsen et al., 2020). Bibi *et al.* demonstrated that the membrane was compatible with the conventional LBDDS digestive conditions in a side-by-side permeation setup in static conditions. While this side-by-side cell-free model was useful for exploring differences in steady-state flux of free versus solubilised drug, the PermeaLoop™ model was developed to better mimic the continuous and dynamic flow conditions in the intestine (Sironi et al., 2018). The Permealoop™ model addressed a shortcoming of the restricted permeation area with the current side-by-side static setup and provided the possibility of using a more physiologically relevant area-to-volume ratio (i.e. 1.38 cm^{-1} A/V), whereby physiological A/V values were estimated to be between 1.9 cm^{-1} and 2.3 cm^{-1} for dissolution evaluation of amorphous solid dispersion of ABT-869 (Berben et al., 2018; Sironi et al., 2018).

The overall aim of the present study was to explore the impact of supersaturation in LBDDS on the permeation and absorption of the model drug celecoxib, relative to 85% saturated LBDDS. To the best of our knowledge, this was the first study to explore impact of sLBDDS versus conventional non-supersaturated LBDDS in combined dispersion/digestion-permeation setups, and under steady-state and dynamic flow conditions. The specific objectives could be summarised as: 1) to compare *in vivo* bioavailability of celecoxib in rats across a range of

supersaturated and non-supersaturated LBDDS; 2) to evaluate the influence of supersaturation, compositional effects and digestive state on permeation across Permeapad® using the side-by-side diffusion cells setup, and 3) to assess supersaturation and compositional effects on drug permeation in a dynamic permeation setup using PermeaLoop™. Finally, in order to improve predictability of the *in vitro* models, *in vitro* conditions were adapted to mimic *in vivo* conditions for pH, bile salts composition, pancreatic enzyme activity and dose:volume considerations for rats.

2. Materials and methods

2.1. Materials

The poorly water-soluble drug used in this study was celecoxib (CCX, weak acid, 381.4 g/mol, logP = 4.3), and was purchased from Astatech Inc. (Bristol, PA, USA). Ibuprofen was used as internal standard for plasma analysis and was obtained from Janssen Pharmaceutica (Beerse, Belgium). Capmul® MCM C8 (medium chain mixed glycerides, MCM) was kindly donated by Abitec (Columbus, OH, USA). Maisine® CC (long chain mono-/di-glycerides, LCM) and Labrasol® ALF (caprylocaproyl polyoxyl-8 glycerides, subsequently denominated as surfactant, S) were kind gifts from Gattefossé (Lyon, France).

Porcine pancreatic lipase 4x USP, calcium chloride dihydrate $CaCl_2 \cdot 2H_20$, 4-bromophenyl-boronic acid (4-BBBA) and maleic acid were purchased from Sigma-Aldrich Denmark ApS (Brøndby, Denmark). Sodium hydroxide was purchased from Merck A/S (Hellerup, Denmark) and polysorbate 80 was acquired from Fluka (Buchs, Switzerland). Purified water was freshly prepared using a Milli-Q® integral water purification system (Milli-Q Advantage A10; MerckMillipore, Merck A/S, Hellerup, Denmark). Rat simulated intestinal fluid (rSIF) powder was prepared according to a publication by Berghausen and co-workers (Berghausen et al., 2016) and had the following components: sodium taurocholate 5 mM, sodium cholate hydrate 12.5 mM, sodium chenodeoxycholic acid 7.5 mM, lecithin 5.16 mM, sodium oleate 0.26 mM and glyceryl monooleate 1.67 mM. Permeapad® phospholipid-based membranes were provided by innoMe (Espelkamp, Germany). All other chemicals and solvents were of analytical or HPLC grade if not stated otherwise and were purchased from VWR (Denmark or Belgium).

2.2. Methods

2.2.1. Design of celecoxib-loaded lipid-based drug delivery systems

Based on initial equilibrium solubility (S_{eq}) measurements of three replicates at 37°C the amounts corresponding to 85% mean S_{eq} (Table 1) were weighed into clean screw-top glass vials and drug-free lipid systems were added up to achieve the target drug concentration. Vials were sealed, mixed and incubated at 37°C for 24 h prior to testing. Similarly, based on S_{eq} measurements at 60°C, supersaturated LBDDS were prepared by adding 85% of $S_{eq}^{60^0C}$ to the lipid systems and heating the mixture at 60°C for 24 h, followed by cooling to ambient temperature. The $S_{eq}^{37^0C}$ and $S_{eq}^{60^0C}$ values of celecoxib in the LCM, MCM and LCM + *S* systems have been reported previously (Ilie et al., 2020a); however, in the case of MCM + *S* systems some modifications had to be made. Firstly, the 80.9 mg/mL value for 85% saturated MCM + *S* is based on an initial solubility triplicate dataset ($S_{eq}^{37^0C}$ = 95 ± 57 mg/mL) which preceded the publication of solubility data (Ilie et al., 2020a). After the *in vivo* study was performed, it was decided that due to high variability, these measurements should be repeated and thus the reported values are as 138 ± 16 mg/mL in the published study (Ilie et al., 2020a). In addition, we found that the freshly prepared sMCM + *S* formulation, prepared with 219.3 mg/mL (i.e. 85% of 258 ± 51 mg/mL) did not produce a clear system, with evidence of drug precipitation after cooling to ambient temperature. Therefore, the actual concentration of the drug in the system (after centrifugation) was determined and reported in Table 1 (128.4 mg/mL). Given the issues observed in this freshly prepared MCM + *S* system, the $S_{eq}^{37^0C}$ was determined again in this specific batch (i.e. 112. 7 ± 6.0 mg/mL). Overall, with these modifications, all final formulations produced clear solutions, with no macroscopic evidence of drug precipitation upon cooling. In addition, drug concentration in the designed (s)LBDDS was confirmed analytically prior to *in vitro* testing. The saturation degree was calculated relative to $S_{eq}^{37^0C}$ and is listed in Table 1 as apparent degree of saturation (aDS) as previously described (Ilie et al., 2020a). Using the above-mentioned values for the MCM + *S* system, the 114% aDS for sMCM + *S* was calculated. Evaluation of the one- and two-component 85% saturated and supersaturated LBDDS was performed in two separate pharmacokinetic rat studies and only the one-component systems were investigated in permeation studies.

2.2.2. Pharmacokinetic evaluation of lipid-based drug delivery systems

The protocol used for the *in vivo* pharmacokinetic evaluation of (s)LBDDS was approved by the institutional animal ethics committee in accordance with the Belgian law regulating animal use in experimental procedures. The study was in compliance with EC Directive 2010/63/EU and the NIH guidelines on animal welfare. Fasted male Sprague-Dawley rats weighing between 250 and 300 g received 0.5 mL/kg celecoxib-loaded 85% saturated or supersaturated LBDDS (n = 4) by oral gavage. Lipid systems were stirred continuously the night before dosing and were clear upon oral administration. 200 µL of whole blood was collected at defined time points: 0.5, 1, 2, 4, 6, 8, 24 h, 100 µL plasma was harvested by centrifugation and bioanalysis was performed on a Waters UPLC™ system with UV-detection. The corresponding dose and aDS for each LBDDS are shown in Table 1. To obtain the absolute bioavailability, celecoxib was also dosed intravenously (i.v.) as an intralipid emulsion (plasma profile not shown). The vehicle of the intralipid emulsion consisted of sesame oil (20.0%, w/w), lecithin (1.2%, w/w), glycerol (2.0%, w/w) and water (76.8%, w/w). Celecoxib, sesame oil and lecithin were mixed and slowly stirred until all celecoxib was dissolved while heating at 60°C. Water and glycerol were mixed and heated at 60°C. When oil phase was ready, the two phases were mixed and homogenised with the IKA T18 digital Ultra Turrax (IKA Works, Inc., NC, USA) at 24 000 rpm for 5 min and the pre-emulsion was then passed through the GEA Panda Plus 200 high pressure homogeniser 2000 (Düsseldorf, Germany) at 1200 bars for 10 cycles.

2.2.2.1. Quantitative analysis of plasma samples. Quantification of celecoxib in plasma after oral dosing of the eight LBDDS was performed using similar reversed-phase UPLC™ (RP-UPLC™) methods

Table 1
Amount corresponding to 85% mean S_{eq}, doses (mg/kg) and apparent degree of saturation (aDS) of orally administered (s)LBDDS.

LBDDS	Composition (w:w)	85% saturated LBDDS			Supersaturated LBDDS		
		Drug concentration (mg/mL)	Dose (mg/kg)	aDS	Drug concentration (mg/mL)	Dose (mg/kg)	aDS
LCM	Long chain mono-/di-glycerides	15.8	7.9	85%	30.8	15.4	166%
MCM	Medium chain mixed glycerides	57.4	28.7	85%	74.8	37.4	110%
LCM + *S*	Long chain mono-/di-glycerides: surfactant (4:1)	62.2	31.1	85%	98.6	49.3	135%
MCM + *S*	Medium chain mixed glycerides: surfactant (4:1)	80.9	40.5	85%	128.4	64.2	114%

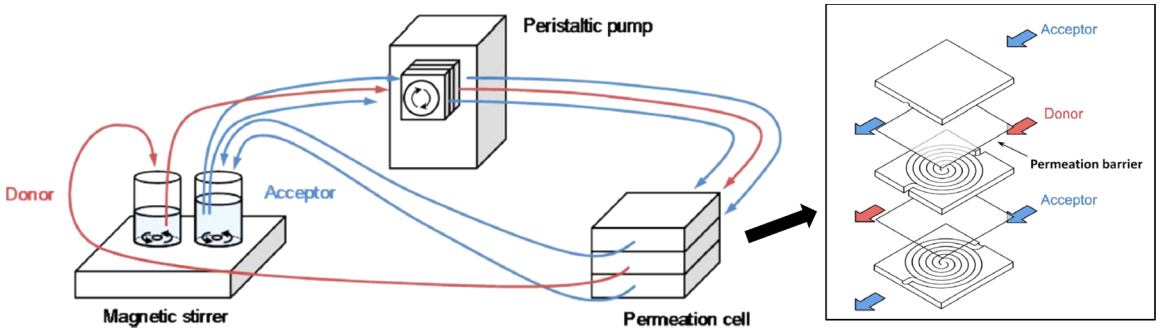

Fig. 1. Schematic representation of PermeaLoop™ model (adapted from Sironi et al.).

with ibuprofen (IBU) as internal standard as indicated by Knopp et al. (Knopp et al., 2016). Ibuprofen was dissolved in acetonitrile to obtain the internal standard solution and 140 µL of this solution was added to 20 µL plasma sample containing celecoxib. Separation of precipitated plasma proteins was successful after centrifugation for 30 min at 17,500 rpm at 4°C using an Eppendorf centrifuge 5430R (Eppendorf, Hamburg, Germany). The concentrations of celecoxib were determined by standard calibration curve analysis using linear fitting of a plot of CCX/IBU peak area ratios versus celecoxib concentrations. The standard calibration curve was linear in the range 10 – 5000 ng/mL and the lowest limit of quantification was 10 ng/mL. A RP Waters Acquity BEH C18, 50 mm × 2.1 mm column packed with 1.7 µm particles (Waters, Milford, USA) was used for the chromatographic analysis with a mobile phase containing a mixture of solvents 0.1% trifluoracetic acid in water: 100% acetonitrile – ACN under a gradient program (0.3 min - 60:40, 2.3 min - 0:100, 2.7 min - 60:40 v:v). The flow rate of the mobile phase was 0.60 mL/min and the injection volume was 2 µL. The column temperature was maintained at 55°C and the wavelength was monitored at 251 nm.

2.2.2.2. Pharmacokinetic and statistical analysis. The primary pharmacokinetic parameters: area under the plasma concentration-time curve (*AUC*), maximum plasma concentration (C_{max}) and time to reach C_{max} (t_{max}) were obtained by non-compartmental analysis of the plasma data, using the linear trapezoidal method in Microsoft Excel (Office 365) with PKSolver add-in. Multiple sample comparison was performed on dose-normalized pharmacokinetic parameters C_{max}, t_{max} and $AUC_{0-24\ h}$ by a two-way analysis of variance (ANOVA) with interaction of two factors (i.e. aDS and LBDDS composition) using SigmaPlot 12.5 from Systat Software, Inc. (Chicago, IL, USA). A *p*-value < 0.05 was considered significant and for statistical contrast analysis, a Tukey post-hoc test was used. Results are expressed as mean ± SD for C_{max} and $AUC_{0-24\ h}$ and median [min, max] for t_{max}.

2.2.3. Permeation studies with lipid-based drug delivery systems

Based on the higher *in vivo* drug exposure as a result of the thermally-induced drug supersaturation and the positive influence of one-component LC LBDDS on *in vivo* performance it was decided to comparatively evaluate the *in vitro* permeation of celecoxib between the supersaturated and non-supersaturated LBDDS composed of only one component (i.e. LCM or MCM). The permeation behaviour of celecoxib LBDDS was firstly evaluated by an *in vitro* passive diffusion experiment across a biomimetic membrane in a setup with side-by-side diffusion cells (PermeaGear Inc., Hellertown PA, USA) at 37°C. The side-by-side setup had a donor volume of 7 mL, an acceptor volume of 5 mL and the effective diffusion area was 1.77 cm^2. The donor phase was represented by either dispersions or digests of the 85% saturated or the supersaturated LCM or MCM formulations containing celecoxib. The preparation of the donor media, dispersed and digested, is described below in Section 2.2.3.2 and 2.2.3.3, respectively. The acceptor medium was represented by an 1% (w/v) Polysorbate 80 (PS80) solution prepared in PBS buffer pH 6.5 to ensure sink conditions. To assemble the permeation setup, the Permeapad® membranes were mounted between the donor and acceptor compartments according to the manufacturer's specifications. Samples from the acceptor compartment were drawn every 30 min over a period of up to 5 h. After every sampling, the acceptor was refilled with 1% PS80 solution to maintain volume and sink conditions. The samples were analysed by UHPLC-UV as described below. The cumulative amount of celecoxib that permeated across the Permeapad® membrane was normalized by the permeation area and plotted against time. From the linear part of this graph the celecoxib steady-state flux was derived ($R^2 > 0.99$ between 1.5 and 5.0 h) (one example in Supplementary information, Figure S1). Additionally, because the concentrations of drug between the different LBDDS, the percentage permeated was calculated as means to normalize between the different doses in the LBDDS according to Eq. (1), where amount in donor is measured at the start of the experiment

$$\%\,\text{permeated} = \frac{Cumulative\ amount\ determined\ in\ the\ acceptor\ compartment\ (t = 5h)}{Amount\ in\ donor\ (dispersed,\ digested)\ (t = 0h)} \quad (1)$$

Steady-state flux values and % permeated were statistically analysed using a one-way ANOVA followed by Tukey's post-hoc test.

Additionally, dispersions of non-supersaturated and supersaturated LCM and MCM were investigated using the PermeaLoop™ model. The setup consists of three parts: donor and acceptor reservoirs (beakers with internal diameter of 3 cm), peristaltic pump, and custom-made permeation cells (Fig. 1). A volume of 20 mL of homogeneous dispersions of (s)LBDDS in rSIF (pH = 6.0) was added in the donor beakers. As acceptor medium, a volume of 35 mL 1% PS80 solution was used to ensure excess solubilization capacity of celecoxib and, thus, sink conditions. Both compartments were stirred continuously at 500 rpm with a rod-shaped stir bar (13 mm × 3 mm) on a multi-position magnetic stirrer (MIXdrive 6 MTP, 2mag AG, Munich,Germany). The media were continuously pumped through the permeation cells at a flow rate of 0.8 mL/min with a peristaltic pump (MCP Standard, Cole-Parmer GmbH, Wertheim, Germany) through TYGON S3™ E-LFL tubes (Ismatec, Wertheim, Germany). Pre-saturation of tubes was done using a 50 µg/mL celecoxib solution in rSIF which was recirculated for 1 h prior to start of experiment.

The custom-made permeation cells consist of three aluminium blocks in which a narrow, spiral-shaped channel has been milled out (Fig. 1). Between each cell, a Permeapad® membrane was mounted, leading to a donor compartment (middle cell) and two acceptor compartments (top and bottom cell). The total permeation area was 27.64 cm^2, and hence, the A/V was 1.38 cm^{-1}. The cells were perfused with a co-current flow and the media were re-circulated into the respective beaker. The permeation study was performed at 37°C in a climate chamber in triplicate. Samples (150 µL) were taken every 30 min for 4 h from the acceptor beaker and replaced with fresh acceptor medium.

The cumulative amount of celecoxib that permeated across the Permeapad® membrane over the 4 h of study in the PermeaLoop™ setup

was calculated and plotted against time (Fig. 4). As suggested before, the percentage permeated was also calculated as means to normalized between the different (s)LBDDS according to Eq. (2) where the amount in donor is measured in the homogeneous dispersion at the start of the experiment.

$$\%\,\text{permeated} = \frac{Cumulative\ amount\ in\ acceptor\ compartment\ (t = 4h)}{Amount\ in\ donor\ (dispersed)\ (t = 0h)} \quad (2)$$

Cumulative amount and % permeated values were statistically analysed using a one-way ANOVA followed by Tukey post-hoc test.

2.2.3.1. Preparation of rat simulated intestinal fluid. Rat simulated intestinal fluid (rSIF) was prepared according to Berghausen et al. who investigating nine compounds with different physico-chemical properties and concluded that the incorporation of rSIF equilibrium solubility values into *in silico* models of oral drug exposure can significantly improve the accuracy of simulations in rats for doses up to 300 mg/kg compared to other media (Berghausen et al., 2016). In short, the solid components (sodium taurocholate, sodium cholate hydrate, sodium chenodeoxycholic acid, lecithin, sodium oleate and glyceryl monooleate) were dissolved in a blend of tert-butanol and water (9:1, w/w) under stirring and gentle warming to 40°C for 1 h (Berghausen et al., 2016). The solution was divided into aliquots, frozen in a freezer (−21 °C), transferred to a pre-cooled freeze-dryer (Christ Gamma 2–16 LSC; Martin Christ GmbH, Osterode am Harz, Germany) with a plate temperature of ≤ −45 °C and freeze dried. During primary drying (overnight), the plate-temperature was steadily to +25 °C while the chamber-pressure was maintained constant at 0.1 mbar. During secondary drying (4 to 8 h), the plate with the vials was maintained at a temperature of 25 °C and the chamber pressure lowered to ≤0.01 mbar. The freeze-dried powder was stored in a desiccator until use. Rehydration was performed with sodium maleate buffer (0.216 g sodium chloride and 0.695 g maleic acid in 200 mL Milli-Q water, pH 2.0), stirred for 24 h at room temperature and finally pH was adjusted to 6.0 with NaOH 0.5 M.

2.2.3.2. Dispersions of lipid-based drug delivery systems. LBDDS at either the 85% or at the supersaturated drug loadings were dispersed in rat SIF (pH 6.0) in a 1:30 ratio to be consistent with the volume administered to the rats (~150 μL/rat) and considering that the volume of intestinal fluid measured in rats in the fasted state would be 4.5 mL based on the reported range by McConnell and co-workers, 3.2 ± 1.8 mL (McConnell et al., 2008). Dispersions were stirred for 10 min at 300 rpm, 37°C to ensure homogeneity prior to transfer to donor diffusion cell or to the PermeLoop™ donor beaker. The total drug concentration (dissolved and dispersed) in this dispersion medium was measured with the UHPLC-UV method described below and used for calculation of percentage permeated.

2.2.3.3. Digestion of lipid-based drug delivery systems. A digestion medium that mimics the rat intestinal conditions was formulated by dissolving $CaCl_2{\cdot}2H_20$ in rat SIF (5 mM) before starting the digestion, instead of continuous addition of Ca^{2+} while digestion progresses, according to a protocol published by Bibi and co-workers (Bibi et al., 2017). Subsequently, the pH was adjusted to 6.5 with NaOH 0.5 M to be consistent with previously tested digestion setups (Bibi et al., 2017). LBDDS were dispersed in the same 1:30 ratio (v:v) as for dispersions described above, in a heated vessel inside of an oven at 37°C.

Digestion was initiated by addition of pancreatin supernatant prepared by suspending the pancreatic extract in rat digestion buffer, which was prepared 10 min prior to use, to limit denaturation. The supernatant was prepared by gentle vortex of the pancreatic extract into rat digestion buffer containing Ca^{2+}. Enough pancreatic extract was added to obtain a rat relevant lipase activity of 179 USP units (USPU/mL) as indicated by Siqueira Jørgensen et al. (Siqueira Jørgensen et al., 2018). When homogenous, the mixture was centrifuged (5804 R centrifuge equipped with a F-34–6–38 rotor, Eppendorf, Hamburg, Germany) at 4000 rpm for 7 min, at 37°C. The supernatant was collected and transferred to the digestion beaker in a 1:9 ratio (v:v), as previously described (Kleberg et al., 2014). In a preliminary digestion study, the pH was monitored to determine the extent of digestion after 1, 2, 3, and 24 h according to a design by Mosgaard et al. and pH values are shown in Table S 1, Supplementary information (Mosgaard et al., 2015). It was concluded that after 1 h digestion most of LCM and MCM LBDDS was digested as a large pH drop was registered in the first hour, followed by a relatively small decrease at latter timepoints. Celecoxib was also quantified in the digests and the concentration was used for calculation of percentage permeated. After each collection of (s)LCM or (s)MCM digests, 4-BBBA was added to inhibit further lipolysis.

2.2.3.4. Celecoxib quantification in donor and acceptor compartments. Quantification of celecoxib was conducted on a Thermo Fisher UltiMate 3000 UHPLC system that was connected to a Diode Array detector and equipped with an RP Kinetex® EVO C18 LC-column (100 × 2.1 mm; particle size 1.7 μm; pore size 100 Å, Phenomenex®). The injection volume was 5 μL, flow rate was set at 0.3 mL/min and the mobile phase consisted of 55% (v/v) purified water containing 0.1% (v/v) trifluoroacetic acid as modifier and 45% (v/v) acetonitrile (isocratic elution). The column oven temperature was set to 40°C. The total run time was 4 min and celecoxib eluted after 2.1 min with a detection wavelength of 251 nm. The method was linear in the range 10 - 5000 ng/mL for side-by-side results and 100 - 10 000 ng/mL for PermeaLoop™ data.

3. Results

3.1. Comparing in vivo bioavailability of supersaturated versus non-supersaturated lipid-based drug delivery systems

A range of supersaturated LBDDS were prepared by adding a fixed amount of drug (based on 85% of $S_{eq}^{60^0C}$, heating to 60°C for 24 h and leaving to cool at ambient temperature prior to oral administration to rats. As outlined in Table 1, aDS ranged between 110 and 166%, depending on the composition. For each formulation, the corresponding non-supersaturated LBDDS was prepared at 85% of the saturation solubility. In general, the aDS of MC systems (i.e. MCM and MCM + *S*) were lower than the aDS for LC systems (i.e. LCM and LCM + *S*). This reflected the higher solubility of the drug in MC systems relative to LC systems and overall lower propensity for thermally-induced supersaturation (Ilie et al., 2020a). In all cases, the dosing volume of 0.5 mL/kg was maintained across all tested lipid systems to ensure the total volume of lipid administered was constant between treatment groups. As a result, the celecoxib dose was different between groups depending on the drug solubility in each system (Table 1). To facilitate direct comparison between the LBDDS in terms of saturation degree and compositional effects, the celecoxib plasma concentrations were dose-normalized (Fig. 2). The corresponding pharmacokinetic parameters are presented in Table 2 and a comparison of dose-normalized $AUC_{0-24\ h}$ plotted against LBDDS composition is illustrated in Fig. 3. Absolute bioavailability (F%) was determined with respect to an i.v. administration (1 mg/kg) of a submicron emulsion with celecoxib (1 mg/g) (n = 4) (mean $AUC_{0-24hr}^{i.v.}$ = 4030 ± 271 ng/mL*h).

With respect to the absorption ($AUC_{0-24\ h}$), thermally-induced supersaturation resulted in a trend towards increasing AUCs for single component systems relative to non-supersaturated systems, which was statistically significant for MCM, but not for LCM. This increase in $AUC_{0-24\ h}$ translated to an increase of 14.5% in the absolute bioavailability for sLCM versus LCM (p = 0.200) and 40.9% for sMCM versus MCM (p = 0.001). An increase in rate of absorption (C_{max}) was also observed for sLCM and sMCM versus their non-supersaturated correspondents, albeit not statistically significant. In terms of t_{max},

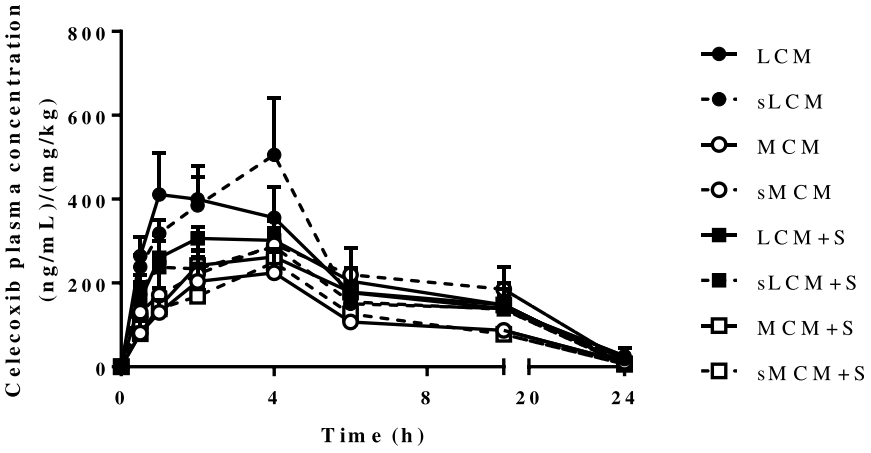

Fig. 2. Plasma concentration-time profiles (mean + SD), $n = 4$ for celecoxib after dosing four LBDDS at 85% drug concentration (continuous lines) and supersaturated drug concentration (interrupted lines). The tested LBDDS were LCM (full circles), MCM (empty circles), LCM + *S* (full squares) and MCM + *S* (empty squares). Data for 85% saturated systems was previously presented in (Ilie et al., 2020b) and are depicted here for comparative purposes with *in vivo* results for supersaturated systems.

statistically significant prolongation was observed for sLCM versus LCM. In surfactant-containing systems no trends were apparent with the extent and rate of absorption being similar between supersaturated and non-supersaturated systems after dose-normalization, with mean absolute bioavailability values of 76.6% and 77.6% for (s)LCM + *S* and 54.7% and 68.9%% for (s)MCM + *S*, respectively.

With regards to compositional effects, the overall observed trend for the extent absorbed increased after administration of LC systems relative to MC systems, which was statistically significant for non-supersaturated systems (LCM and MCM), but not for sLBDDS (sLCM and sMCM). The better *in vivo* performance of the LCM system, either non-supersaturated or supersaturated, is also shown by the rate of absorption which showed statistically significantly higher C_{max} values relative to the corresponding MC systems (MCM and MCM + *S*). Furthermore, a statistically significant increase was identified for C_{max} and $AUC_{0-24\ h}$ of sLCM and for $AUC_{0-24\ h}$ of sMCM relative to surfactant-containing sMCM + *S*. Finally, the statistical evaluation confirmed an interaction between the two factors aDS and composition for $AUC_{0-24\ h}$ and absolute bioavailability. Therefore, this may indicate that the *in vivo* effects are the result of interplay between the factors and not just individual factors.

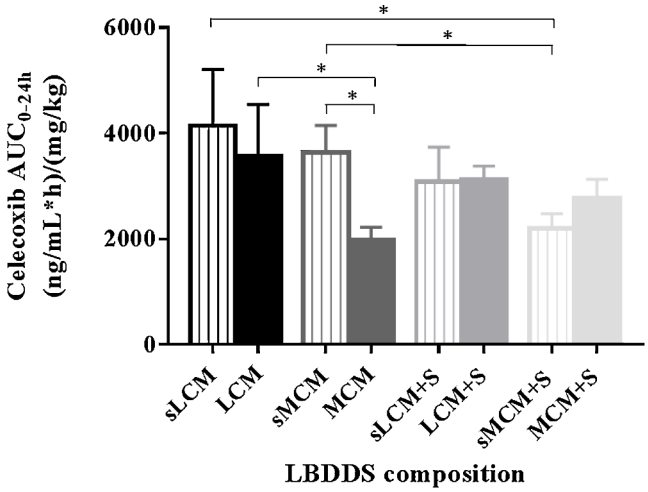

Fig. 3. Dose-normalized area under the concentration-time plasma profiles (mean + SD) obtained after oral administration of (s)LBDDS containing celecoxib ($n = 4$)). Full bars represent 85% saturated LBDDS and bars with lines represent supersaturated LBDDS. Statistics represent pairwise comparison. Data for 85% saturated systems was previously presented in (Ilie et al., 2020b) and are depicted here for comparative purposes with *in vivo* results for supersaturated systems.

3.2. Influence of supersaturation, compositional effects and digestive state on in vitro steady-state permeation across Permeapad®

The mean celecoxib steady-state flux of (s)LCM and (s)MCM systems

Table 2
Dose-normalized pharmacokinetic parameters C_{max}, $AUC_{0-24\ h}$ (mean ± SD) and t_{max} (median, [min, max]) following single oral administration of LBDDS at 85% saturated or supersaturated celecoxib ($n = 4$). Statistics represent pairwise comparisons.

LBDDS	LCM		MCM		LCM + S		MCM + S	
aDS	85% saturated	Supersaturated	85% saturated	Supersaturated	85% saturated	Supersaturated	85% saturated	Supersaturated
C_{max} (ng/mL)	429 ± 78[a]	506 ± 137[b]	237 ± 52[a]	308 ± 19[b]	325.6 ± 7.1	286.7 ± 69.7[b]	270 ± 63[a]	249 ± 43.3[b]
AUC $_{0}$-24 h (ng/mL*h)	3563.5 ± 984.5[c]	4145 ± 1062[d]	1978.6 ± 243.6[c,f]	3626.2 ± 519.8[e,f]	3126.6 ± 251.3	3085.2 ± 651.3	2776 ± 354	2203 ± 274[d,e]
t_{max} (h)	1.5 [1.0; 4.0][g]	4.0 [4.0; 4.0][g]	4.0 [2.0; 4.0]	4.0 [2.0; 8.0]	3.0 [1.0; 4.0]	4.0 [4.0; 4.0]	3.0 [2.0; 4.0]	4.0 [4.0; 4.0]
F (%)	88 ± 21[h]	103 ± 23[i]	49.1 ± 5.2[h,k]	90 ± 11[j,k]	77.6 ± 5.4	77 ± 14	68.9 ± 7.6	54.7 ± 5.9[i,j]

[a] C_{max}: LCM statistically significant from MCM and MCM + *S* (85% saturated);.
[b] C_{max}: sLCM statistically significant from all other tested supersaturated LBDDS;
[c] AUC_{0-24h}: LCM statistically different from MCM (85% saturated);.
[d] AUC_{0-24h}: sLCM statistically different from sMCM + *S* (supersaturated);.
[e] AUC_{0-24h}: sMCM statistically different from sMCM + *S*;.
[f] AUC_{0-24h}: sMCM statistically different from MCM;
[g] t_{max}: sLCM statistically significant longer relative to LCM.
[h] F: LCM statistically significant from MCM (85% saturated);.
[i] F: sLCM statistically significant from sMCM + *S* (supersaturated);.
[j] F: sMCM statistically significant from sMCM + *S* (supersaturated);.
[k] F: sMCM statistically different from MCM. Calculated i.v. $AUC_{0-24\ h}$ value was 4030 ± 271 ng/mL*h.

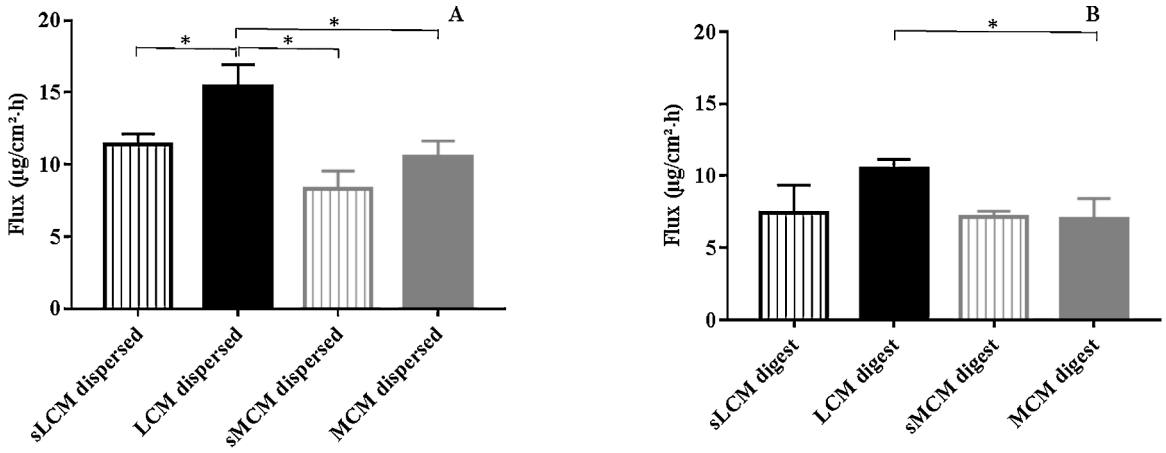

Fig. 4. Side-by-side permeation data of celecoxib LBDDS at 85% or supersaturated drug loadings either as dispersed (A) or digested (B) versions of the drug delivery systems in rat simulated intestinal fluid using a biomimetic Permeapad® permeation membrane. Results shown as mean + SD and statistics represent multiple pairwise comparison in the dispersions and digests groups.

in a side-by-side setup across Permeapad® is presented in Fig. 4 (A, dispersions and B, digests). A general trend towards lower flux values for supersaturated LBDDS was observed relative to their corresponding non-supersaturated systems, and in the case of sLCM versus LCM the difference was statistically significant ($p < 0.05$). In terms of compositional effects, the flux of LCM dispersion was statistically higher relative to MCM, sLCM and sMCM dispersions (Fig. 4A). In addition, in the post-digested state drug flux for the LCM system was also statistically higher relative to MCM digest (Fig. 4B). Additionally, another compositional effect was observed for the precipitation propensity between LC and MC systems, with drug precipitate evident on dispersion of the MC systems, whereas no drug precipitation was visible for LC systems.

As an alternative to comparing flux parameters, given that the dose loading varied between LBDDS, the total amount and % of drug permeated across the membrane into the acceptor compartment after 5 h was calculated, relative to the concentration of drug at the beginning of the experiment (Table 3). Allowing for the different doses, calculation of % permeated indicated that the supersaturated systems did not increase permeation, with no significant differences observed between the sMCM relative to MCM system (0.008 ± 0.004% and 0.004 ± 0.001% for dispersions and 0.005 ± 0.001% and 0.004 ± 0.001% after digestion). Similar to the observations based on flux, the % permeated was lower for the sLCM relative to LCM (0.010 ± 0.003% and 0.015 ± 0.006% respectively as dispersions), albeit not significant in this case. In terms of compositional effects, % drug permeated from LCM and sLCM were generally higher (non-significant) than for the corresponding MC systems which is in line with flux observations.

Subsequently, digestion effect was assessed using simulated digestion conditions that mimic *in vivo* conditions in the rat. It was apparent that for all four (s)LBDDS, the flux was higher when dispersions of the lipid systems were used in the donor compartment of the side-by-side setup in comparison to the respective pancreatin-digested lipid systems. Statistical differences were found for both non-supersaturated LCM and MCM with higher flux values from dispersions compared to digested versions (Table 3). The statistically significant compositional effect of higher flux from LCM versus MCM was also identified in the digested state.

3.3. *In vitro* dynamic drug permeation across Permeapad® membrane in Permealoop™

The dynamic PermeaLoop™ model can achieve continuous flow of donor and acceptor media in the system and thus ensure dynamic flow-through conditions for better assessment of interplay between dispersion/digestion and permeation. A plot of the cumulative amount permeated as a function of time and the calculated % permeated after 4 h are illustrated in Fig. 5 and Table 4, respectively. The advantage of higher surface area for permeation resulted in higher amount and % drug permeated relative to the static conditions. The results illustrated that under dynamic flow conditions the supersaturation state did not increase the % permeated for sMCM (3.2 ± 0.4%) versus MCM (2.7 ± 0.7%), which was in line with observations from the side-by-side model. A reduction in permeation was also observed with dynamic conditions for sLCM relative to LCM (6.0 ± 2.0% and 11.9 ± 5.2%). With regards to compositional effects both at non-supersaturated and supersaturated aDS, utilisation of LC systems resulted in higher drug permeated (as percentage of dose) relative to the MC systems. A statistically significant difference was identified for LCM compared to MCM and sMCM. This further supported the fact that % permeated

Table 3
Permeation data (flux, amount permeated, % permeated) obtained during side-by-side permeation studies with dispersion and digests of 85% saturated and supersaturated LBDDS. Statistics represent multiple pairwise comparison to identify differences between dispersions and digests in either non-supersaturated or supersaturated LBDDSs.

LBDDS	Dispersions			Digests		
	Flux (μg/cm²·h)	Amount permeated (μg)	% permeated (5 h)	Flux (μg/cm²·h)	Amount permeated (μg)	% permeated (5 h)
sLCM	11.4 ± 0.8	0.6 ± 0.2	0.010 ± 0.003	7.4 ± 1.9	1.3 ± 0.9	0.018 ± 0.013
LCM	15.4 ± 1.5[a]	0.5 ± 0.2	0.015 ± 0.006	10.4 ± 0.7[a,c]	0.6 ± 0.0	0.015 ± 0.001
sMCM	8.3 ± 1.3	1.7 ± 0.8	0.008 ± 0.004	7.1 ± 0.4	1.0 ± 0.1	0.005 ± 0.001
MCM	10.6 ± 1.1[b]	0.6 ± 0.1	0.004 ± 0.001	7.0 ± 1.5[a,b,c]	0.7 ± 0.1	0.004 ± 0.001

[a] Flux: LCM dispersion statistically different from LCM digest, MCM dispersed and MCM digest.
[b] Flux: MCM dispersion statistically different from MCM digest.
[c] Flux: LCM digest statistically different from MCM digest.

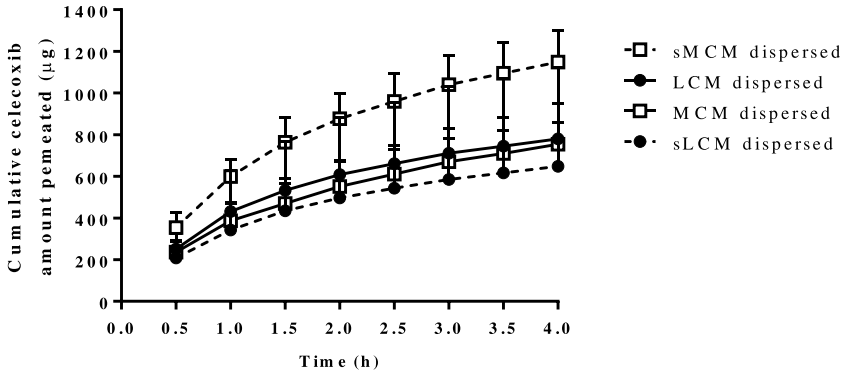

Fig. 5. Graphical representation of the amount permeated in time across the Permeapad® membrane in a dynamic dispersion-permeation study using PermeaLoop™.

Table 4
Amount permeated and corresponding %permeated obtained after evaluation of dynamic dispersion-permeation PermeaLoop™ model of dispersions of 85% saturated and supersaturated LBDDS containing celecoxib.

LBDDS	Amount permeated (µg)	% permeated (4 h)
sLCM	648 ± 212	6.0 ± 2.0
LCM	780 ± 342	11.9 ± 5.2[a]
sMCM	1149 ± 152	3.2 ± 0.4[a]
MCM	754 ± 194	2.7 ± 0.7[a]

[a] LCM % permeated statistically significantly higher than MCM and sMCM.

under dynamic conditions allowed for a better comparison given the use of different doses between LBDDS.

4. Discussion

Increasing drug loadings in LBDDS by thermally-induced supersaturation has resulted in improved bioavailability for some drugs in preclinical pharmacokinetic studies. However, studies that have evaluated sLBDDS using the common lipolysis pH-stat *in vitro* methods, have failed to show the potential to improve *in vivo* performance using supersaturated systems relative to a non-supersaturated system (Thomas et al., 2014; Siqueira et al., 2017). This suggests a limitation for the standard single stage digestion model, and that there is a need to further investigate the effects of sLBDDS using bio-predictive *in vitro* models that combine both dispersion/digestion of LBDDS with an absorptive sink. In this study, the performance of LBDDS at either non-supersaturated or supersaturated drug loadings were tested *in vivo* in rats and *in vitro* using two novel models with the Permeapad® permeation membrane. Compositional effects such as differences in fatty acid chain length were also evaluated *in vitro* and *in vivo* and addition of surfactant in composition of LC and MC LBDDS was assessed *in vivo*.

Typically, *in vivo* performance of sLBDDS has been investigated using a well-studied complex lipid system consisting of 4 excipients (triglycerides, blends of mono-/di-glycerides, surfactant and co-solvent). Therefore, the majority of studies reported in the literature comparing non-supersaturated and supersaturated LBDDS have used the same drug dose, which resulted in administration of less lipid volume in the case of sLBDDS (Siqueira et al., 2017; Michaelsen et al., 2016; Thomas et al., 2014). Nevertheless, administration of a lower amount of lipid in the formulation may underpredict the benefits of supersaturated systems given the direct participation of LBDDS components in generation and maintenance of an increased solubilization capacity for PWSD upon dispersion in GI fluids. In contrast, the present work focused on the head-to-head *in vivo* comparison of four LBDDS consisting of either single or two components LBDDS and the subsequent administration of the same lipid volume. The limitation of such approach was that the dose of drug was variable, depending on the solubility in lipids, why the data needed to be dose-normalized. Using this experimental approach, overall, supersaturation had a significant positive effect on celecoxib exposure after administration of supersaturated sLCM and sMCM systems relative to non-supersaturated systems. Therefore, this study demonstrated the merits of higher drug loaded sLBDDS for increasing exposure of drug, which could be particularly relevant for preclinical safety and toxicology studies. Dose increases of 1.9-fold or 1.3-fold for single component LC and MC systems resulted in increases of 2.3 and 2.4-fold in drug exposure (calculations before dose-normalization of $AUC_{0–24\ h}$). Addition of surfactant resulted in minimal exposure benefits at either drug loadings. Nevertheless, the supersaturation approach may still be useful in early preclinical safety studies, given the simplicity of the studied systems for rapid screening of a dose range. Overall, the study showed that using a low-technology input (i.e. heating to 60°C) for formulation of supersaturated lipid systems, formulation scientists are able to load higher doses of a PWSD in compositionally simple formulations and can achieve increased exposure upon oral administration.

In order to gain additional mechanistic understanding into the supersaturation and composition effects on the interplay between dispersion/digestion and permeation, the (s)LCM and (s)MCM systems were assessed in a side-by-side permeation setup using the biomimetic membrane Permeapad®. Interestingly, our findings indicated that supersaturated LBDDS did not increase drug flux, but rather paradoxically decreased steady-state flux relative to equivalent non-supersaturated LBDDS. In the case of LCM systems, the flux of the supersaturated system was statistically lower than the flux of non-supersaturated system. Possible reasons why the LCM system, which contained the lowest drug load and thus lowest total drug concentration, displayed the highest flux were unclear, but may reflect that upon dispersion of such a system, the drug will be dissolved either freely (i.e. molecularly dissolved) or solubilized within the colloidal assemblies that form. Higher flux for the LCM system may reflect that this dispersion was favourable for maintaining free drug concentrations in the aqueous medium, which continues to permeate across the membrane. In contrast, increasing the dose loading, as in the case of supersaturated LCM, did not lead to further increases in flux. This may indicate that the relative amount of free drug in the aqueous media of supersaturated systems was lower than in non-supersaturated systems. Alternatively, despite higher total drug concentrations for the sLCM systems, due to higher partitioning of drug within the colloidal oil droplets, the supersaturated system did not readily maintain the free drug concentrations in the aqueous medium under conditions of ongoing drug permeation. Therefore, further studies at different dose loading are required to delineate if the increased dose load due to supersaturation results in proportionate increases in both free and colloidally associated drugs on dispersion.

This study also explored compositional effects to increase drug exposure and showed that LC systems increased celecoxib bioavailability over MC systems at both non-supersaturated and supersaturated dose loadings. In contrast, addition of surfactant had no positive influence on

celecoxib exposure at the two dose loadings. Looking at the impact of composition on permeation in this side-by-side setup flux and % permeated results would indicate that LCM systems yielded higher overall permeation relative to MCM systems. This was observed in both dispersed and digested states and was statistically significant for non-supersaturated systems, i.e. LCM relative to MCM.

The relatively small area-to-volume ratio (i.e. 0.25 cm^{-1}) of the side-by-side setup was likely to be a factor in the relatively low overall values for % drug permeated (between 0.004 ± 0.001% and 0.018 ± 0.013%). The low A/V ratio was also regarded as a main limitation of the setup, which may also be a factor in the lack of significant differences observed between the various formulations tested i.e. limited ability to differentiate between formulations under low A/V steady-state flux conditions. Therefore, the PermeaLoop™ setup, with a higher A/V ratio of 1.38 cm^{-1}, offered additional insights into the influence of drug supersaturation and compositional effects on celecoxib permeation in a dynamic dissolution-permeation setup. Overall, the % permeated values were higher (between 2.7 ± 0.7% and 11.9 ± 5.2%) than in the side-by-side setup. The PermeaLoop™ model was generally in line with the steady-state model, i.e. supersaturation increased flux for the MCM system, but overall, no significant differences were observed for the supersaturation effects in the dynamic model. In terms of compositional effects, the dynamic flow model revealed similar observations to both the *in vivo* data and the static model; however, in contrast to the static model it revealed the statistically significant higher LCM % permeation, with 11.9 ± 5.2% of the dose appearing in the acceptor media after 4 h, compared to 2.7 ± 0.7% for the MCM system ($p = 0.017$) and 3.2 ± 0.4% for sMCM ($p = 0.022$) (Table 4).

Digestion is believed to play an important role in absorption processes of PWSD from LBDDS, which has guided research towards establishing increasingly complex lipolysis models (Iwanaga et al., 2006; Yeap et al., 2013; Berthelsen et al., 2019). In the present study, the difference in celecoxib permeability between dispersions and digests of LCM and MCM was also assessed in a steady-state diffusion setup using conditions that simulated the rat intestine. Results indicated that a higher flux was obtained in the dispersed state of either non-supersaturated or supersaturated LBDDS, compared to corresponding digested states. The results indicated statistically significant differences between LCM dispersions (15.4 ± 1.6) and digests (10.4 ± 0.7) and between MCM dispersions (10.6 ± 1.1) and digests (6.9 ± 1.5). This could be a result of increased solubilization capacity of the post-digestive state, where digested lipids served to increase solubilisation capacity of bile salt-lipid micelles, which could overall reduce the available fraction of free drug that can further permeate across the membrane. In support of this, higher apparent solubilities of celecoxib were observed in simulated digested LCM and MCM biorelevant media relative to dispersed lipids (Ilie et al., 2020b). Similarly, a recent observation by Jacobsen et al. indicated a higher solubilisation capacity for celecoxib by monoacyl-phospholipids as compared to diacyl-phospholipids, the former representing the lipolytic degradation product of the latter, which was in line with the outlined hypothesis of increased solubilisation in media with lipolytic end-products (Jacobsen et al., 2019). Collectively therefore, this may suggest that the post-digestive conditions may lead to lower steady-state flux, at least in models where the lipids/surfactant molecules do not readily permeate across the membrane. These observations may lend further support to the concept of developing digestion-independent or 'stealth' LBDDS to increase drug absorption (Feeney et al., 2014).

While the overall flux was lower under simulated digestive conditions, the higher flux from the LCM system was still maintained relative to the MCM system under post-digestive state. Biorelevant solubility determinations showed higher solubilisation capacity of celecoxib in simulated post-digestive MCM systems, compared to LCM equivalents (Ilie et al., 2020b). Therefore, it appeared that the higher solubilization capacity in the colloidal environment did not directly translate to increased permeation across the biomimetic membrane. The higher flux observed for LC systems may in part explain the improved *in vivo* bioavailability observed for LCM systems. Alternatively, the relatively poor performance of MCM systems may have reflected a higher precipitation risk from MC systems as observed in a study by Sek et al. whereby MC blends of mono-/di-glycerides were rapidly digested, forming an aqueous dispersed phase or a precipitated fraction (Sek et al., 2002). In contrast, LC blends of glycerides were more slowly digested, the undigested oily phase still being present throughout the 30-minutes digestion (Sek et al., 2002). A similar higher propensity for precipitation in MCM versus LCM systems was visually observed in the donor compartment in the present study.

Relating *in vitro* results to *in vivo* data has been a strong focus of research groups over the past decades. In the present study, a first attempt to relate *in vitro* permeation data from two different models to *in vivo* results obtained after administration of non-supersaturated and supersaturated LBDDS was made and is summarized in Table 5. Using the steady-state model, flux did not anticipate the better *in vivo* performance of supersaturated LBDDS compared to non-supersaturated systems and the dose-normalised data (i.e. % permeated) suggested a trend towards higher permeation for supersaturated systems, though no overall significant differences were observed ($p > 0.05$). In contrast, the compositional effects seen *in vivo* were predicted based on the higher flux of LC systems over MC systems. Similarly, the higher permeability effect of LCM versus MCM (3.8-fold for both dispersions and digests) and sLCM versus sMCM (1.3-fold for dispersions and 3.6-fold for digests) was evident when comparing % permeated at steady-state. Digestion was shown to have a negative impact on flux of tested (s)LBDDS and overall had a limited benefit *in vitro* testing also considering the increased resource and time investment needed to run this experimental design. Therefore, while it is desirable to create *in vivo*-adapted biopharmaceutical *in vitro* models, it may also be useful during early

Table 5
Summary of findings after *in vivo* and *in vitro* evaluation of non-supersaturated (85%) and supersaturated lipid-based drug delivery systems containing celecoxib.

		In vivo	Permeapad®		PermeaLoop™
		AUC	Flux	% perm	% perm
Supersaturation	sMCM versus MCM	Y ($p < 0.05$)	N	Y ($p > 0.05$)	Y($p > 0.05$)
	sLCM versus LCM	Y ($p > 0.05$)	N*	N	N
Composition	LCM versus MCM	Y ($p < 0.05$)	Y ($p < 0.05$)	Y ($p > 0.05$)	Y ($p < 0.05$)
	sLCM versus sMCM	Y ($p > 0.05$)	Y ($p > 0.05$)	Y ($p > 0.05$)	Y ($p > 0.05$)
	MCM + *S*/LCM + *S* versus MCM/LCM	N	N/A	N/A	N/A
Digestion	sMCM versus MCM	N/A	Y ($p > 0.05$)	Y ($p > 0.05$)	N/A
	sLCM versus LCM		N	Y ($p > 0.05$)	
	LCM versus MCM		Y ($p < 0.05$)	Y ($p > 0.05$)	
	sLCM versus sMCM		Y ($p > 0.05$)	Y ($p > 0.05$)	

Y = yes effect observed (± statistically significant difference); *N* = no effect observed;.
N* = statistically significant opposite effect; N/*A* = not applicable.

stage drug development to assess the *in vitro* performance of bio-enabling lipid formulations with more simplistic (i.e. without digestive conditions) models which have predictive potential for *in vivo* performance. A first attempt was outlined in this study in terms of using the rat biorelevant rat media, readily available dispersions of (s)LBDDS and dynamic flow conditions maintained by the PermeaLoop™ model. With this new model, a different permeation profile was observed compared to a steady-state setup (Figure S1 and Fig. 5). The statistically significant difference observed between LCM and MCM % permeated was correctly identified with the dynamic model. During a dispersion-permeation study, steady-state conditions were observed if the permeation was rate limiting. In the case of PermeaLoop™ the cumulated amount permeated curve deviated from a straight line and tended asymptotically towards a constant value. This suggested that the amount permeated was highly dependant on the release of free drug from the formulation, which was especially relevant for bio-enabling formulations such as LBDDS. Further developments to the model are encouraged in terms of optimization of flow rates, dilution volumes, pH adjustments, dispersion and acceptor media, in order to improve robustness and bio-relevance of the model.

5. Conclusions

The present study demonstrated that at equivalent lipid doses, increasing the drug saturation above equilibrium solubility resulted in an increased *in vivo* bioavailability of celecoxib from single component LBDDS relative to the corresponding non-supersaturated LBDDS. Using the *in vitro* Permeapad® model, while supersaturation in LBDDS did not reveal higher flux across the biomimetic membrane, the beneficial impact of LCM system versus MCM system was observed, similar to observations *in vivo*. This study demonstrated the utility to explore digestion-permeation, with studies demonstrating that steady-state flux was lower under post-digestive conditions, but compositional difference was still evident. Possible reasons for this may reflect the dynamic interplay between molecularly dissolved drug and colloidally associated drug, and the associated impact on steady-state permeation through the membrane. Proof-of-concept studies in the PermeaLoop™ dynamic flow model confirmed a statistically significantly higher % permeated for LC versus comparable MC systems, which would suggest that % permeated was a more useful parameter to compare formulations than the steady-state flux. Overall, these *in vivo* and *in vitro* studies provided a framework for demonstrating the utility of dispersion/digestion-permeation models to explore the dynamic and complex solubility-permeation interplay in (s)LBDDS. Further studies on supersaturation and/or compositional approaches to maximise permeation under both steady-state and dynamic flow are merited.

CRediT authorship contribution statement

Alexandra-Roxana Ilie: Conceptualization, Data curation, Formal analysis, Investigation, Methodology, Project administration, Resources, Software, Visualization, Writing - original draft, Writing - review & editing. **Brendan T. Griffin:** Conceptualization, Funding acquisition, Project administration, Resources, Supervision, Visualization, Writing - review & editing. **Martin Brandl:** Conceptualization, Methodology, Project administration, Resources, Supervision, Writing - review & editing. **Annette Bauer-Brandl:** Conceptualization, Methodology, Project administration, Resources, Supervision, Writing - review & editing. **Ann-Christin Jacobsen:** Conceptualization, Methodology, Resources, Software, Writing - review & editing. **Maria Vertzoni:** Conceptualization, Funding acquisition, Supervision, Visualization, Writing - review & editing. **Martin Kuentz:** Conceptualization, Funding acquisition, Supervision, Visualization, Writing - review & editing. **Ruzica Kolakovic:** Conceptualization, Supervision, Writing - review & editing. **René Holm:** Conceptualization, Data curation, Funding acquisition, Project administration, Resources, Supervision, Visualization, Writing - review & editing.

Acknowledgments

Alexandra-Roxana Ilie, Brendan T. Griffin, Maria Vertzoni, Martin Kuentz, Ruzica Kolakovic and René Holm are part of the PEARRL European Training network, which has received funding from the Horizon 2020 Marie Sklodowska-Curie Innovative Training Networks programme under grant agreement No. 674909. The current collaboration has been established during a meeting facilitated by UNGAP (Cost action CA18205). The personnel in the animal facility at Janssen Pharmaceutica (Beerse, Belgium) is highly acknowledged for their skillful handling of animals. The research group at University of Southern Denmark is highly acknowledged for offering comprehensive practical trainings to PhD student Alexandra-Roxana Ilie.

Supplementary materials

Supplementary material associated with this article can be found, in the online version, at doi:10.1016/j.ejps.2020.105452.

References

Alskär, L.C., Parrow, A., Keemink, J., Abrahamsson, B., Bergström, C.A.S., 2019. Effect of lipids on absorption of carvedilol in dogs: is coadministration of lipids as efficient as a lipid-based formulation? J. Control. Release. https://doi.org/10.1016/j.jconrel.2019.04.038.

Anby, M.U., Nguyen, T.-.H., Yeap, Y.Y., Feeney, O.M., Williams, H.D., Benameur, H., Pouton, C.W., Porter, C.J.H., 2014. An *in vitro* digestion test that reflects rat intestinal conditions to probe the importance of formulation digestion vs first pass. doi:10.1021/mp500197b.

Berben, P., Bauer-Brandl, A., Brandl, M., Faller, B., Flaten, G.E., Jacobsen, A.C., Brouwers, J., Augustijns, P., 2018. Drug permeability profiling using cell-free permeation tools: overview and applications. Eur. J. Pharm. Sci. https://doi.org/10.1016/j.ejps.2018.04.016.

Berghausen, J., Seiler, F.H., Gobeau, N., Faller, B., 2016. Simulated rat intestinal fluid improves oral exposure prediction for poorly soluble compounds over a wide dose range4, 35–53. doi:10.5599/admet.4.1.258.

Berthelsen, R., Klitgaard, M., Rades, T., Müllertz, A., 2019. *In vitro* digestion models to evaluate lipid based drug delivery systems; present status and current trends. Adv. Drug Deliv. Rev. 29–35. https://doi.org/10.1016/j.addr.2019.06.010.

Bibi, H.A., Holm, R., Bauer-Brandl, A., 2017. Simultaneous lipolysis/permeation *in vitro* model, for the estimation of bioavailability of lipid based drug delivery systems. Eur. J. Pharm. Biopharm. 117, 300–307. https://doi.org/10.1016/j.ejpb.2017.05.001.

Buckley, S.T., Frank, K.J., Fricker, G., Brandl, M., 2013. Biopharmaceutical classification of poorly soluble drugs with respect to “enabling formulations.”. Eur. J. Pharm. Sci. 50, 8–16. https://doi.org/10.1016/j.ejps.2013.04.002.

Christfort, J.F., Strindberg, S., Plum, J., Hall-Andersen, J., Janfelt, C., Nielsen, L.H., Müllertz, A., 2019. Developing a predictive *in vitro* dissolution model based on gastrointestinal fluid characterisation in rats. Eur. J. Pharm. Biopharm. 142, 307–314. https://doi.org/10.1016/j.ejpb.2019.07.007.

Dahan, A., Miller, J.M., Hoffman, A., Amidon, G.E., Amidon, G.L., 2010. The solubility–permeability interplay in using cyclodextrins as pharmaceutical solubilizers: mechanistic modeling and application to progesterone. J. Pharm. Sci. 99, 2739–2749. https://doi.org/10.1002/jps.22033.

Di Cagno, M., Bibi, H.A., Bauer-brandl, A., 2015. New biomimetic barrier Permeapad ™ for efficient investigation of passive permeability of drugs. Eur. J. Pharm. Sci. 73, 29–34. https://doi.org/10.1016/j.ejps.2015.03.019.

Feeney, O.M., Crum, M.F., McEvoy, C.L., Trevaskis, N.L., Williams, H.D., Pouton, C.W., Charman, W.N., Bergström, C.A.S., Porter, C.J.H., 2016. 50 years of oral lipid-based formulations: provenance, progress and future perspectives. Adv. Drug Deliv. Rev. 101, 167–194. https://doi.org/10.1016/j.addr.2016.04.007.

Feeney, O.M., Williams, H.D., Pouton, C.W., Porter, C.J.H., 2014. ‘ Stealth ’ lipid-based formulations : poly (ethylene glycol) -mediated digestion inhibition improves oral bioavailability of a model poorly water soluble drug. J. Control. Release 192, 219–227. https://doi.org/10.1016/j.jconrel.2014.07.037.

Fischer, S.M., Brandl, M., Fricker, G., 2011a. Effect of the non-ionic surfactant Poloxamer 188 on passive permeability of poorly soluble drugs across Caco-2 cell monolayers. Eur. J. Pharm. Biopharm. 79, 416–422. https://doi.org/10.1016/j.ejpb.2011.04.010.

Fischer, S.M., Flaten, G.E., Hagesæther, E., Fricker, G., Brandl, M., 2011b. *In-vitro* permeability of poorly water soluble drugs in the phospholipid vesicle-based permeation assay: the influence of nonionic surfactants. J. Pharm. Pharmacol. 63, 1022–1030. https://doi.org/10.1111/j.2042-7158.2011.01301.x.

Frank, K.J., Westedt, U., Rosenblatt, K.M., Hölig, P., Rosenberg, J., Mägerlein, M., Brandl, M., Fricker, G., 2012. Impact of FaSSIF on the solubility and dissolution-/permeation rate of a poorly water-soluble compound. Eur. J. Pharm. Sci. 47, 16–20. https://doi.org/10.1016/j.ejps.2012.04.015.

Griffin, B.T., Kuentz, M., Vertzoni, M., Kostewicz, E.S., Fei, Y., Faisal, W., Stillhart, C., O'Driscoll, C.M., Reppas, C., Dressman, J.B., 2014. Comparison of *in vitro* tests at various levels of complexity for the prediction of *in vivo* performance of lipid-based formulations: case studies with fenofibrate. Eur. J. Pharm. Biopharm. 86, 427–437. https://doi.org/10.1016/j.ejpb.2013.10.016.

Holm, R., 2019. Bridging the gaps between academic research and industrial product developments of lipid-based formulations. Adv. Drug Deliv. Rev. https://doi.org/10.1016/j.addr.2019.01.009.

Ilie, A.-R., Griffin, B.T., Kolakovic, R., Vertzoni, M., Kuentz, M., Holm, R., 2020a. Supersaturated lipid-based drug delivery systems–exploring impact of lipid composition type and drug properties on supersaturability and physical stability. Drug Dev. Ind. Pharm. 46, 356–364. https://doi.org/10.1080/03639045.2020.1721526.

Iwanaga, K.I., Ushibiki, T.K., Iyazaki, M.M., Akemi, M.K., 2006. Disposition of lipid-based formulation in the intestinal tract affects the absorption of poorly water-soluble drugs Biol. Pharm. Bull. 29, 508–512.

Jacobsen, A.-.C., Nielsen, S., Brandl, M., Bauer-Brandl, A., 2020. Drug permeability profiling using the novel Permeapad® 96-well plate. Pharm. Res. 37, 93. https://doi.org/10.1007/s11095-020-02807-x.

Ilie, A.-R., Griffin, Brendan T., Vertzoni, M., Kuentz, M., Cuyckens, F., Wuyts, K., Kolakovic, R., Holm, R., 2020b. Towards simplified oral lipid-based drug delivery using mono-/di-glycerides as single component excipients. Submitt. Drug Dev. Ind. Pharm.

Jacobsen, A.C., Elvang, P.A., Bauer-Brandl, A., Brandl, M., 2019. A dynamic *in vitro* permeation study on solid mono- and diacyl-phospholipid dispersions of celecoxib. Eur. J. Pharm. Sci. 127, 199–207. https://doi.org/10.1016/j.ejps.2018.11.003.

Keemink, J., Mårtensson, E., Bergström, C.A.S., 2019. Article a lipolysis-permeation setup for simultaneous study of digestion and absorption *in vitro*. doi:10.1021/acs.molpharmaceut.8b00811.

Kleberg, K., Maio, M., Jannin, V., Igonin, A., Partheil, A., Marchaud, D., Jule, E., Vertommen, J.A.N., E, R.I.C.C., Ullertz, A.M., Christopher, J.H., 2014. Toward the establishment of standardized *in vitro* tests for lipid-based formulations, Part 1 : method parameterization toward the establishment of standardized *in vitro* tests for lipid-based formulations, Part 1 : method parameterization and comparison. doi:10.1002/jps.23205.

Knopp, M.M., Nguyen, J.H., Mu, H., Langguth, P., Rades, T., Holm, R., 2016. Influence of copolymer composition on *in vitro* and *in vivo* performance of celecoxib-PVP/VA amorphous solid dispersions. AAPS J. 18, 416–423. https://doi.org/10.1208/s12248-016-9865-6.

McConnell, E.L., Basit, A.W., Murdan, S., 2008. Measurements of rat and mouse gastrointestinal pH, fluid and lymphoid tissue, and implications for *in-vivo* experiments63–70. doi:10.1211/jpp.60.1.0008.

Michaelsen, M.H., Wasan, K.M., Sivak, O., Müllertz, A., Rades, T., 2016. The effect of digestion and drug load on halofantrine absorption from self-nanoemulsifying drug delivery system (SNEDDS). AAPS J. 18, 180–186. https://doi.org/10.1208/s12248-015-9832-7.

Mosgaard, M.D., Sassene, P., Mu, H., Rades, T., Müllertz, A., 2015. European journal of pharmaceutics and biopharmaceutics development of a high-throughput *in vitro* intestinal lipolysis model for rapid screening of lipid-based drug delivery systems. Eur. J. Pharm. Biopharm. 94, 493–500. https://doi.org/10.1016/j.ejpb.2015.06.028.

Müllertz, A., Ogbonna, A., Ren, S., Rades, T., 2010. New perspectives on lipid and surfactant based drug delivery systems for oral delivery of poorly soluble drugs. J. Pharm. Pharmacol. 62, 1622–1636. https://doi.org/10.1111/j.2042-7158.2010.01107.x.

O'Dwyer, P.J., Box, K.J., Koehl, N.J., Bennett-Lenane, H., Reppas, C., Holm, R., Kuentz, M., Griffin, B.T., 2020. A novel biphasic lipolysis method to predict *in vivo* performance of lipid based formulations. Submitt. Mol. Pharm.

Savla, R., Browne, J., Plassat, V., Wasan, K.M., Wasan, E.K., 2017. Review and analysis of FDA approved drugs using lipid-based formulations. Drug Dev. Ind. Pharm. 0, 1–16. https://doi.org/10.1080/03639045.2017.1342654.

Sek, L., Porter, C.J.H., Kaukonen, A.M., Charman, W.N., 2002. Evaluation of the *in-vitro* digestion pro les of long and medium chain glycerides and the phase behaviour of their lipolytic products 29–41.

Siqueira Jørgensen, S.D., Al Sawaf, M., Graeser, K., Mu, H., Müllertz, A., Rades, T., 2018. The ability of two *in vitro* lipolysis models reflecting the human and rat gastro-intestinal conditions to predict the *in vivo* performance of SNEDDS dosing regimens. Eur. J. Pharm. Biopharm. 124, 116–124. https://doi.org/10.1016/j.ejpb.2017.12.014.

Siqueira, S.D.V.S., Müllertz, A., Gräeser, K., Kasten, G., Mu, H., Rades, T., 2017. Influence of drug load and physical form of cinnarizine in new SNEDDS dosing regimens: *in vivo* and *in vitro* evaluations. AAPS J. 19. https://doi.org/10.1208/s12248-016-0038-4.

Sironi, D., Rosenberg, J., Bauer-brandl, A., Brandl, M., 2018. Journal of pharmaceutical and biomedical analysis PermeaLoop TM, a novel *in vitro* tool for small-scale drug-dissolution/permeation studies. J. Pharm. Biomed. Anal. 156, 247–251. https://doi.org/10.1016/j.jpba.2018.04.042.

Thomas, N., Holm, R., Garmer, M., Karlsson, J.J., Müllertz, A., Rades, T., 2013. Supersaturated self-nanoemulsifying drug delivery systems (Super-SNEDDS) enhance the bioavailability of the poorly water-soluble drug simvastatin in dogs. AAPS J. 15, 219–227. https://doi.org/10.1208/s12248-012-9433-7.

Thomas, N., Holm, R., Mullertz, A., Rades, T., 2012. *In vitro* and *in vivo* performance of novel supersaturated self-nanoemulsifying drug delivery systems (super-SNEDDS). J. Control. Release 160, 25–32. https://doi.org/10.1016/j.jconrel.2012.02.027.

Thomas, N., Richter, K., Pedersen, T.B., Holm, R., Müllertz, A., Rades, T., 2014. *In vitro* lipolysis data does not adequately predict the *in vivo* performance of lipid-based drug delivery systems containing fenofibrate. AAPS J. 16, 539–549. https://doi.org/10.1208/s12248-014-9589-4.

Williams, Trevaskis, N.L., Charman, S.A., Shanker, R.M., Charman, W.N., 2013. Strategies to address low drug solubility in discovery and development 315–499.

Yeap, Y.Y., Trevaskis, N.L., Quach, T., Tso, P., Charman, W.N., Porter, C.J.H., 2013. Intestinal bile secretion promotes drug absorption from lipid colloidal phases via induction of supersaturation. doi:10.1021/mp3006566.